

Phonon dispersions of cluster crystals

Tim Neuhaus¹ and Christos N Likos^{2‡}

¹ Institute of Theoretical Physics, Heinrich Heine University of Düsseldorf,
Universitätsstraße 1, D-40225 Düsseldorf, Germany

² Faculty of Physics, University of Vienna, Boltzmanngasse 5, A-1090 Vienna, Austria

Abstract. We analyze the ground states and the elementary collective excitations (phonons) of a class of systems, which form cluster crystals in the absence of attractions. Whereas the regime of moderate-to-high-temperatures in the phase diagram has been analyzed in detail by means of density functional considerations (Likos C N, Mladek B M, Gottwald D and Kahl G 2007 *J. Chem. Phys.* **126** 224502), the present approach focuses on the complementary regime of low temperatures. We establish the existence of an infinite cascade of isostructural transitions between crystals with different lattice site occupancy at $T = 0$ and we quantitatively demonstrate that the thermodynamic instabilities are bracketed by mechanical instabilities arising from long-wavelength acoustical phonons. We further show that all optical modes are degenerate and flat, giving rise to perfect realizations of Einstein crystals. We calculate analytically the complete phonon spectrum for the whole class of models as well as the Helmholtz free energy of the systems. On the basis of the latter, we demonstrate that the aforementioned isostructural phase transitions must terminate at an infinity of critical points at low temperatures, brought about by the anharmonic contributions in the Hamiltonian and the hopping events in the crystals.

PACS Numbers: 64.70.Dv, 61.20.Ja, 82.30.Nr, 82.70.Dd

1. Introduction

Particles interacting by means of bounded and purely repulsive interaction potentials $v(r)$ can form cluster crystals at sufficiently high densities [1, 2, 3, 4, 5, 6, 7, 8, 9]. Though the existence of clustering in the full absence of attractions might seem counterintuitive at first, its existence rests on solid mathematical and physical grounds and has also been amply demonstrated by means of detailed computer simulations [2, 10, 11]. A necessary and sufficient condition for the occurrence of clustering is that the Fourier transform of the interaction potential, $\tilde{v}(k)$, has negative parts. In this case, the properties of the system, both in the liquid and in the crystal phases, are largely determined by the position of the wavevector, k_* , at which $\tilde{v}(k)$ attains its most negative value and by the negative amplitude $-|\tilde{v}(k_*)|$ of the Fourier spectrum of the potential there [3]. The physical realizability of such potentials as *effective interactions* between suitably tailored

‡ Corresponding author, E-mail address: christos.likos@univie.ac.at

macromolecules has been demonstrated for the case of amphiphilic dendrimers as well as ring polymers [12, 13].

At moderate to high temperatures, the thermodynamics of the system is very accurately described by a mean-field density functional theory, which predicts, among other properties, that the lattice constant of the crystal is density-independent [3]. This is brought about by the mechanism of occupying the crystal sites by a multiple number of particles n_c which scales proportionally to the density of particles, ρ , in the crystal. Within this crystal, the equilibrium dynamics of the particles is characterized by two kinds of processes: the first one, operating at short time scales, is determined by lattice oscillations. At the same time, there is incessant particle hopping between sites, which brings about an overall average occupancy n_c per site. The latter process is activated, diffusive dynamics, which brings about a self-diffusion coefficient of the particles that scales as $\exp(-\psi\rho/T)$, where T is the absolute temperature and ψ is a coefficient that depends on the precise form of the interaction potential [14].

Whereas the diffusive, long-time dynamics of the clustered crystals is by now well-understood due to a number of different studies, the phonon dynamics, which is the dominant one at very low temperatures, has not been analyzed in detail. Similarly, whereas the phase behavior of the system at moderate to high temperatures is very thoroughly examined, little is known regarding the phase diagram of the system at very low temperatures. The analysis of the elementary excitations (phonons) in the cluster crystals opens a route to low-temperature thermodynamics as well, since it allows for the calculation of the free energy of the system on the basis of a harmonic lattice theory. The purpose of this paper is precisely to calculate and analyze the phonon spectra of cluster crystals and to draw, on this basis, conclusions on the stability, dynamics and thermodynamics of these systems at low temperatures. We find that cluster crystals have very unusual, yet simple, phonon spectra, in which all optical modes are degenerate and the optical frequencies are independent of the wavenumber, rendering thereby these solids into perfect Einstein crystals. Further, we discover a cascade of mechanical instabilities in the system, initiated at the long-wavelength limit of the low-lying acoustical modes, which trigger an avalanche of isostructural phase transitions from crystals of occupancy n_c to crystals of occupancy $n_c + 1$, whereby n_c is an integer number. Finally, we predict that the (infinitely many) density gaps associated with the isostructural transitions at $T = 0$ gradually close up as T grows and they terminate at critical points at low temperatures.

The rest of the manuscript is organized as follows: In sec. 2 we calculate the zero-temperature phase diagram, to establish the ground states on which the phonon spectra have to be determined. The calculation of the phonon curves follows then in sec. 3 and the ensuing phonon-based phase diagram of the system in sec. 4. Finally, in sec. 5 we summarize and draw our conclusions.

2. Zero-temperature phase diagram

To set up the stage and gather the key results for the system, we commence with the definition of the relevant quantities and a collection of hitherto known results. We consider a system of N particles in a volume V , which interact via a bounded and positive interaction potential $v(r)$:

$$0 \leq v(r) < \infty. \quad (1)$$

The system is characterized by its density $\rho = N/V$ as well as the absolute temperature T . Without loss of generality, we can introduce an energy scale ε and a length scale σ that set the strength and range of the potential $v(r)$, respectively, writing the latter in the form:

$$v(r) = \varepsilon\phi(r/\sigma), \quad (2)$$

with some dimensionless function $\phi(z)$ of a dimensionless argument z . Accordingly, one can define the scaled density $\rho^* \equiv \rho\sigma^3$ as well as the scaled temperature $T^* \equiv k_B T/\varepsilon$, where k_B is Boltzmann's constant. Another crucial quantity is the Fourier transform $\tilde{v}(k)$ of $v(r)$, which contains negative parts, i.e., $v(r)$ belongs to what has been termed the Q^\pm class of interactions [1]. In particular, we consider its most negative value, which is assumed at the wavenumber k_* :

$$-|\tilde{v}(k_*)| = \min_k \tilde{v}(k). \quad (3)$$

At temperatures $T^* \gtrsim 0.1$, analytical considerations and comparisons with extensive computer simulations have shown that the system forms clustered crystals with the following properties [2, 3, 4, 10]. First, the freezing line (T_f, ρ_f) from a fluid (at low densities) to the cluster crystal (at high densities) takes, approximately, the form:

$$k_B T_f \approx 1.393|\tilde{v}(k_*)|\rho_f. \quad (4)$$

Second, the clustered crystals feature an average lattice site occupancy n_c that scales as

$$n_c = \frac{8\sqrt{2}\pi^3}{k_*^3}\rho, \quad (5)$$

resulting into a density-independent lattice constant a of the crystal. Finally, the long-time, diffusive dynamics of the crystals is determined by an activated-hopping mechanism, resulting into a diffusivity D that is given by [14]:

$$D \cong [(\psi\rho^*/T^*)^2/2 + \psi\rho^*/T^* + 1] \exp(-\psi\rho^*/T^*), \quad (6)$$

with a potential-dependent coefficient ψ .

As is clear from eq. (5) above, the average occupancy n_c of the lattice is a general, real number. At any instant, of course, every crystal site is occupied by some integer number of particles. At finite temperatures, the activated hopping mechanism that brings about the long-time diffusivity D of eq. (6), constantly redistributes particles between instantaneous 'donor' and 'acceptor' sites, bringing about the aforementioned average occupancy n_c . At $T = 0$, however, this mechanism is absent, therefore each

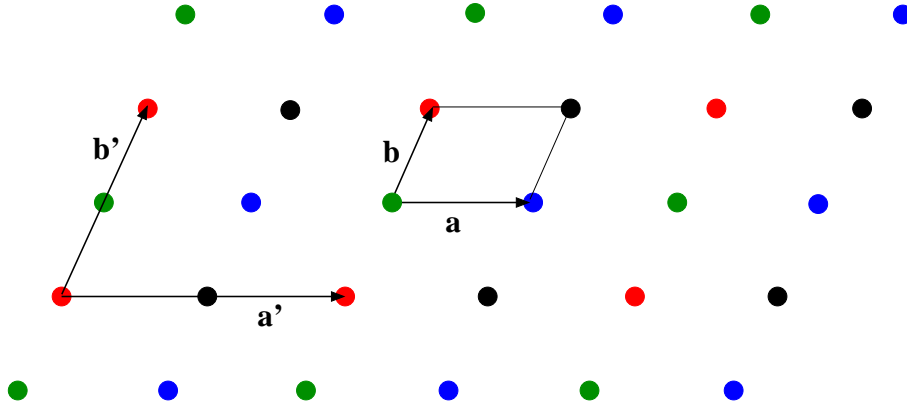


Figure 1. A schematic demonstration of the procedure to generate the most general decorated lattice (here in two dimensions) that fulfills inversion symmetry (see the text). The underlying Bravais lattice is spanned by the elementary vectors \mathbf{a} and \mathbf{b} . The vertices of the elementary unit cell, denoted by the parallelogram, are decorated by clusters of different occupancy, marked by the four different colors. Afterwards, the decorated cell is flipped along the sides generated by the vectors \mathbf{a} and \mathbf{b} . The procedure is repeated for every new decorated unit cell until the whole lattice is filled.

site has an occupancy that is frozen-in. In addition, the zero-temperature phase has to fulfill the strict requirement of *mechanical equilibrium*§ on each and every lattice site, i.e., the *force* exercised on every particle on the lattice site, due to the rest of the crystal must vanish. This immediately excludes the possibility of a periodic crystal with arbitrarily varying occupancies between the lattice sites: inversion symmetry of the decorated crystal structure must be guaranteed, so that mechanical equilibrium can result.

The most general way of achieving this is depicted in Fig. 1. One takes the elementary unit cell of the lattice and decorates each vertex with (in general different) integer occupancies of the lattice sites. Then, the cell is ‘flipped’ along the axes defined by the elementary vectors and the process is repeated until the whole lattice is filled. For the two-dimensional case shown for purposes of clarity in Fig. 1, the resulting structure can also be regarded as a crystal with a unit cell spanned by the vectors $\mathbf{a}' = 2\mathbf{a}$ and $\mathbf{b}' = 2\mathbf{b}$, accompanied by a four-membered basis at the vectors $\mathbf{B}_1 = 0$, $\mathbf{B}_2 = \mathbf{a}$, $\mathbf{B}_3 = \mathbf{b}$, and $\mathbf{B}_4 = \mathbf{a} + \mathbf{b}$. The generalization to three dimensions is straightforward, where one obtains up to eight sublattice occupancies n_i , $i = 1, 2, \dots, 8$ and the corresponding overall occupancy of the lattice is a *rational* number:

$$n_c = \frac{1}{8} \sum_{i=1}^8 n_i. \quad (7)$$

§ Mechanical equilibrium is a necessary condition for stability of a structure, not a sufficient one; the increasingly stronger requirements of mechanical and thermodynamic stability must also be fulfilled for a phase to be materialized. The question of the mechanical stability of this equilibrium will be discussed in sec. 3.

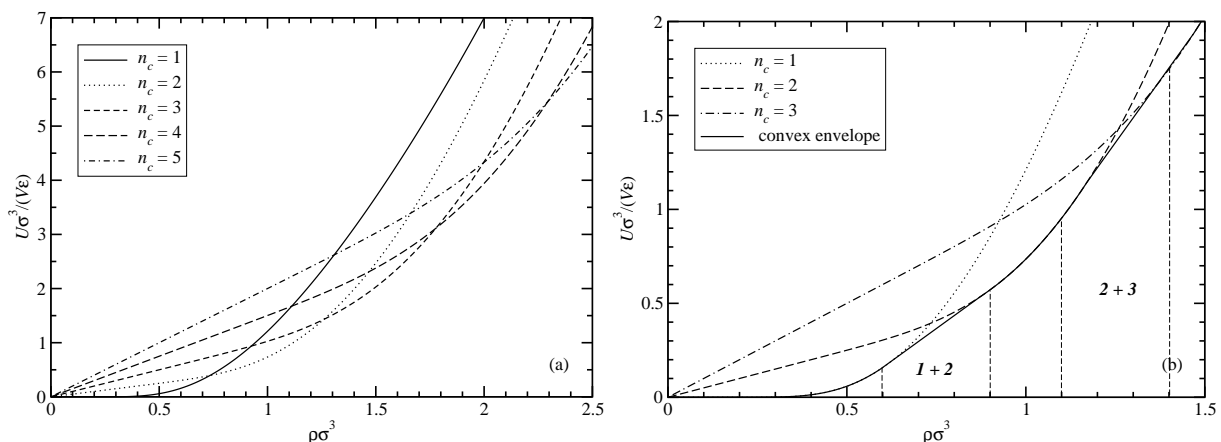


Figure 2. (a) The internal energy density U/V of GEM4 fcc crystals with successively high occupancies per lattice site, n_c , as a function of the density ρ . The occupancies are indicated in the legend. (b) A zoom on the lower density part of (a), showing also the convex reconstruction of the curves and the resulting two-phase coexistence regions between crystals with successive occupancy numbers. The coexistence regions correspond to the straight-line segments of the U/V vs. ρ -curves and are also marked by the vertical broken lines. The inscriptions in these regions denote the occupancies of the coexisting crystals.

Evidently, even this combinatorial freedom does not restore the general possibility of real (i.e., in general irrational) n_c numbers present for $T \neq 0$. For the concrete example of the interaction potential examined in the rest of the paper, we checked a few possible combinations of n_i 's at selected densities and we found that the most stable lattice decoration at $T = 0$ is the one in which *all* n_i 's coincide. On these grounds, and on the basis of parsimony and clarity, we will consider in the rest of the paper precisely only the case for which every lattice site is occupied by the same, integer number of particles. Thus, we will be discussing crystals of single, double, triple, etc. occupancy.

Though a host of results to be derived below are quite general for all potentials in the Q^\pm class, we are working with the generalized exponential model with exponent 4, GEM4, described by the interaction potential:

$$v(r) = \epsilon \exp[-(r/\sigma)^4]. \quad (8)$$

At $T = 0$, the stable crystal lattice for this potential is fcc, as confirmed earlier by applying a very efficient search among all Bravais lattices via a genetic algorithm approach [2, 15]. The ground-state phase diagram is determined by the configurations that minimize the internal energy U (the lattice sum). In particular, one has to minimize the internal energy density U/V and the latter must be a convex function of the particle density ρ of the system.

Results are shown in Fig. 2. In Fig. 2(a) it can be seen that with increasing density, crystals with occupancy n_c become thermodynamically less favorable and they give their place to crystals with occupancy $n_c + 1$. At the same time, regions of non-convexity appear around the points on which the U/V vs. ρ -curves of the various occupancies

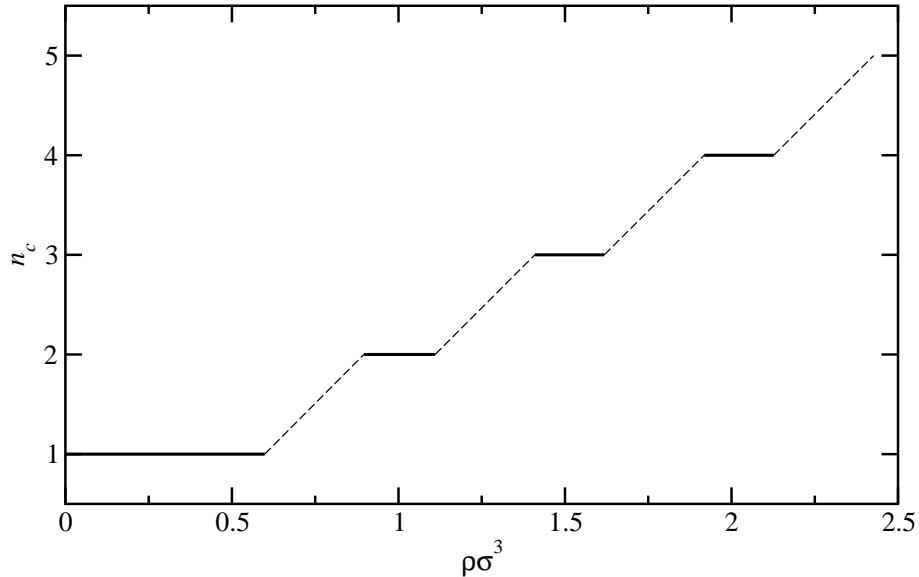


Figure 3. The zero-temperature dependence of the lattice occupancy n_c of GEM4 fcc crystals on their density. The thick horizontal lines lie in single-phase density regions, separated by phase-coexistence density gaps, denoted by the thin broken lines.

cross. These have to be made convex by means of the common tangent construction, as shown in Fig. 2(b), giving rise to regions of coexistence between the crystal of occupancy n_c and the crystal of occupancy $n_c + 1$. In what follows, we denote with $\rho_{n_c/n_{c+1}}^-$ and $\rho_{n_c/n_{c+1}}^+$ the lower and upper density boundaries of the coexistence region between the fcc solids of occupancy n_c and $n_c + 1$. For consistency in the notation, let us also define $\rho_{0/1}^+ = 0$. The phase behavior of the system at $T = 0$ can be summarized as follows. For $\rho_{n_{c-1}/n_c}^+ \leq \rho^* \leq \rho_{n_c/n_{c+1}}^-$ a single crystal of occupancy n_c is stable, whereas for densities ρ^* in the range $\rho_{n_c/n_{c+1}}^- < \rho^* < \rho_{n_c/n_{c+1}}^+$, a macrophase separation between the crystals of successive occupancies n_c and $n_c + 1$ takes place.

In Fig. 3 we show the dependence of the $T = 0$ site occupancy n_c on density. The characteristic step-like structure that emerges is a signature of the ground state and a precursor of the $n_c \propto \rho$ dependence, eq. (5), encountered for higher temperatures. Indeed, the ‘smoothing-out’ of the steplike form of the occupancy into a continuous, straight line is brought about by the hopping mechanism mentioned above. The ranges of stability of the n_c -occupied crystals and the associated regions of coexistence for the fcc GEM4-crystals at zero temperature are summarized in Table 1 for the first few values of n_c .

In Fig. 4, we show the resulting dependence of the lattice constant a of the fcc crystals on their density. Within the regions $\rho_{n_{c-1}/n_c}^+ \leq \rho^* \leq \rho_{n_c/n_{c+1}}^-$, in which a pure crystal with occupancy n_c is stable, the lattice constant decreases with density as $a = \gamma(n_c/\rho)^{1/3}$, with some geometric prefactor γ . In the regions $\rho_{n_c/n_{c+1}}^- < \rho^* < \rho_{n_c/n_{c+1}}^+$, we have the coexistence between two crystals, one with occupancy n_c and lattice constant $a^- = \gamma(n_c/\rho_{n_c/n_{c+1}}^-)^{1/3}$, and one with occupancy $n_c + 1$ and lattice constant

Table 1. The density ranges of stability of the n_c -occupied fcc GEM4 crystals, shown here up to the coexistence region between quintuple and sextuple occupied solids. The symbols ‘ $a + b$ ’ on the left column, where $b = a + 1$, denote, as in the figures, the regions of macroscopic coexistence (phase separation) between crystals of occupancy n_c and $n_c + 1$.

Site occupancy n_c	Density range ρ^*
1	0 - 0.5985
1 + 2	0.5985 - 0.8961
2	0.8961 - 1.1100
2 + 3	1.1100 - 1.4094
3	1.4094 - 1.6182
3 + 4	1.6182 - 1.9179
4	1.9179 - 2.1267
4 + 5	2.1267 - 2.4267
5	2.4267 - 2.6336
5 + 6	2.6336 - 2.9336

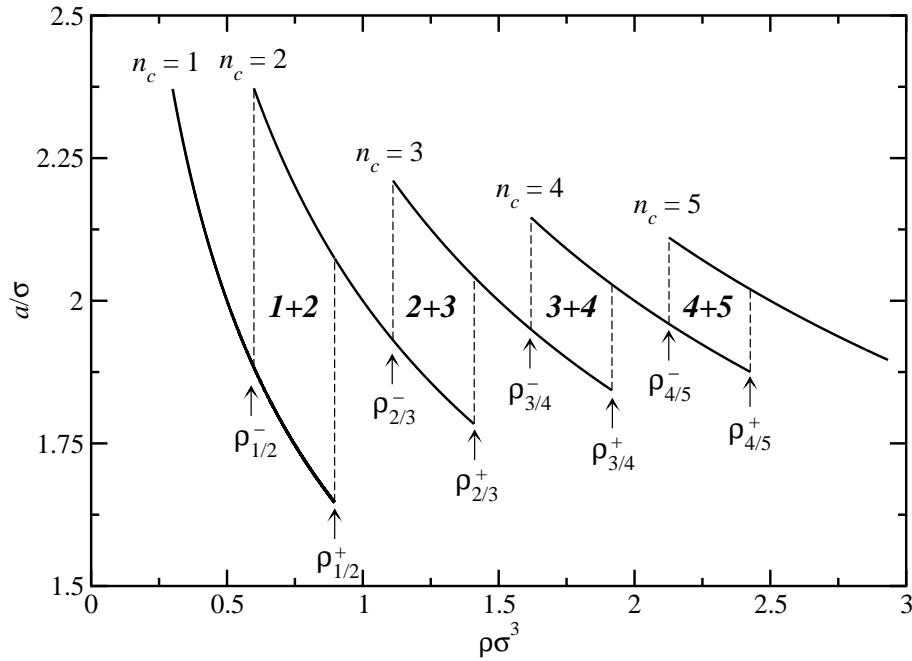


Figure 4. The zero-temperature dependence of the lattice constant a of GEM4 fcc crystals on their density. The thick solid lines have the dependence $a = \gamma(n_c/\rho)^{1/3}$ and they are artificially extended beyond the range of stability of single phases, within the coexistence regions, for purposes of demonstration. The coexistence regions are denoted by thin vertical lines and the inscriptions in those denote the occupancies of the two coexisting crystals. The lower- and upper densities of the coexistence gaps are marked with arrows. For the overall, reconstructed dependence of a on density, taking phase coexistences properly into account, see the text.

$a^+ = \gamma((n_c + 1)/\rho_{n_c/n_c+1}^+)^{1/3}$. Whereas for a crystal of single occupancy the lattice constant would monotonically decrease with density as $\rho^{-1/3}$, here we see already at $T = 0$ the propensity of the cluster crystals to suppress the variation of a with ρ . This comes about through the growth of n_c with ρ in two complementary fashions: on the one hand, for the single phase regions, the relative difference between $(n_c/\rho)^{1/3}$ and $((n_c + 1)/\rho)^{1/3}$ shrinks as n_c grows. On the other hand, the intervening two-phase coexistence regions have the effect that, although the lattice constant decreases with ρ within a single-phase region, it gets ‘kicked up’ again when the transition to the next single-phase region takes place. Indeed, as can be seen in Fig. 4, the range of variation of a with density becomes increasingly narrower as ρ , and thus also n_c grow. Once again, this is the $T = 0$ precursor of the ensuing density-independence of a on ρ that has been established for higher temperatures. The way in which the discontinuous change of n_c and/or a with density at zero temperature evolve into the smooth curves at higher temperature will be discussed in sec. 4.

3. Phonon spectra and stability analysis

3.1. Single occupancy crystals

The calculation of the phonons spectra, once the ground states have been determined, follows along standard ways [16]. The particles are subjected to small deviations around their equilibrium lattice positions $\{\mathbf{R}\}$, denoted by the displacement field $\mathbf{u}(\mathbf{R})$, and the total interaction energy is split into the lattice sum U and a harmonic potential U^{harm} , which is a quadratic form of $\mathbf{u}(\mathbf{R})$:

$$U^{\text{harm}} = \frac{1}{2} \sum_{\mathbf{R}} \sum_{\mathbf{R}'} \mathbf{u}(\mathbf{R}) \mathbf{D}(\mathbf{R} - \mathbf{R}') \mathbf{u}(\mathbf{R}'), \quad (9)$$

where the dynamical matrix $\mathbf{D}(\mathbf{R} - \mathbf{R}')$ has the elements

$$D_{\alpha\beta}(\mathbf{R} - \mathbf{R}') = \frac{\partial^2 U^{\text{harm}}}{\partial u_{\alpha}(\mathbf{R}) \partial u_{\beta}(\mathbf{R}')}, \quad (10)$$

α, β denoting Cartesian coordinates. Determination of the phonon spectrum $\omega(\mathbf{k})$ results from diagonalization of the matrix

$$\mathbf{D}(\mathbf{k}) = \sum_{\mathbf{R}} \mathbf{D}(\mathbf{R}) \exp[-i\mathbf{k} \cdot \mathbf{R}]. \quad (11)$$

In particular, the eigenvalues of the matrix $\mathbf{D}(\mathbf{k})$ are equal to $m\omega^2(\mathbf{k})$, m being the particle mass.

The phonon spectra have been calculated along the $\Gamma \rightarrow X \rightarrow W \rightarrow K \rightarrow \Gamma$ -path in the first Brillouin zone of the fcc-lattice, shown in Fig. 22.13(b) of Ref. [16]. We note, in particular, that the $\Gamma \rightarrow X$ section of this path corresponds to wavevectors \mathbf{k} along the [100] direction of the cubic crystal, whereas the last part of the path, $K \rightarrow \Gamma$, to wavevectors along the [110] direction, which is also the nearest-neighbor vector in the fcc crystal. The points X and K lie at the edges, whereas the point Γ at the center of the Brillouin zone.

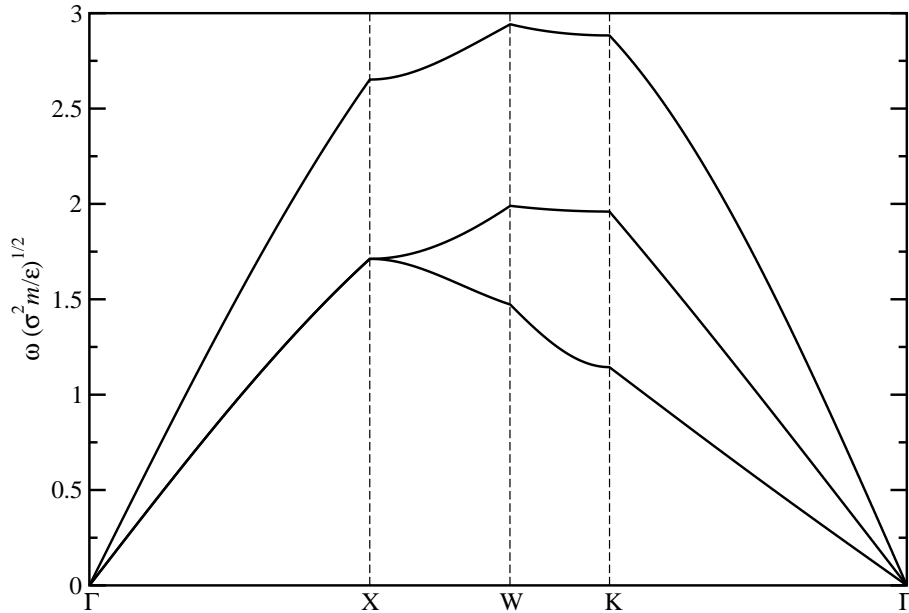


Figure 5. The phonon spectrum of the single occupied fcc GEM4-crystal at density $\rho^* = 0.5$.

The phonon spectrum of the single occupied fcc GEM4-crystal at density $\rho^* = 0.5$ is shown in Fig. 5. Along the high-symmetry, $\Gamma \rightarrow X$, $[100]$ direction, we find, as expected, two degenerate transverse acoustical branches, as well as a separate longitudinal branch. The degeneracy of the two former ones is lifted along the other directions in the Brillouin zone. Upon increasing the density of the crystal, starting at vanishingly small values, the slope of the lowest branch in the $\Gamma \rightarrow K$ direction has a nonmonotonic behavior. It first increases and then starts decreasing again, a development that is at odds with that for usual, monatomic crystals. The decrease of the slope results, at a density $\rho_{x,1}^*$ at the appearance of a *negative eigenvalue*, which corresponds to an imaginary frequency and thus signals a *mechanical instability* of the crystal. We have numerically found for $\rho_{x,1}^*$ the value

$$\rho_{x,1}^* = 0.7205. \quad (12)$$

Since the instability first occurs at the point Γ , i.e., for $k = 0$, it signals a propensity of the single occupied crystal to undergo a long-wavelength transformation (compression/expansion), fully consistent with the thermodynamic instability towards the formation of a doubly occupied crystal with a different lattice constant. Referring to Table 1, we see that the point of mechanical instability lies above the point of thermodynamic instability, $\rho_{1/2}^- = 0.5985$, of the single occupied crystal. In other words, the incipient mechanical instability of the system, at which the slightest perturbation to the crystal will result into its collapse, is *preempted* by a first-order transition to a doubly occupied crystal. The scenario is reminiscent of the first-order freezing transition of the cluster fluid into the cluster crystal preempting the instability line at $k = k_*$, encountered for the very same systems [1, 2, 3], the difference being that the latter occurs at finite

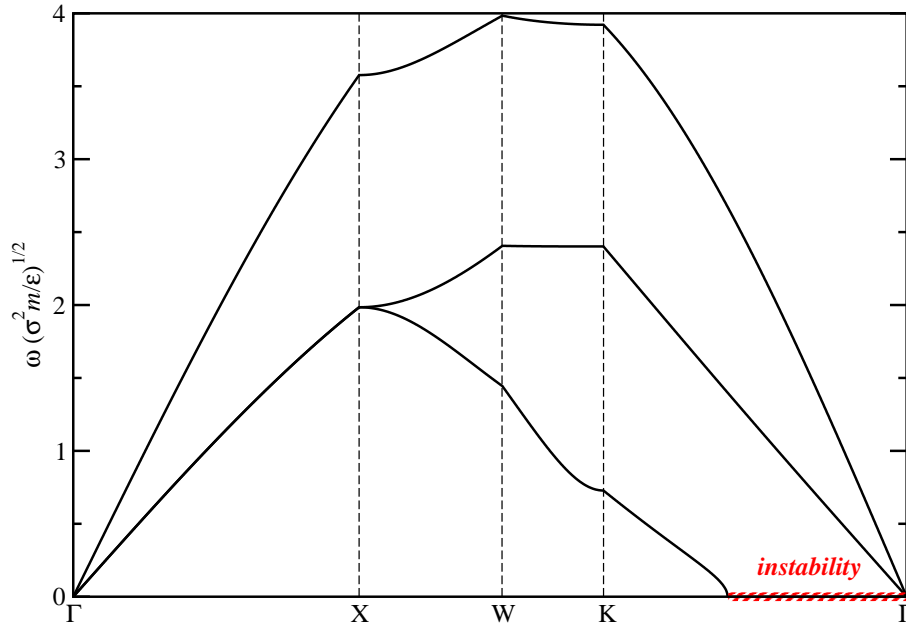


Figure 6. The phonon spectrum of the single occupied fcc GEM4-crystal at density $\rho^* = 0.75$. The cross-hatched region on the horizontal axis denotes the values of wavenumbers for which the matrix $\mathbf{D}(\mathbf{k})$ has negative eigenvalues.

values of the wavenumber and signals thus an ordering with finite wavelength. At any rate, the fact that the thermodynamic phase transition precedes the mechanical instability is the only consistent scenario, since the opposite would lead to an obvious contradiction. Upon further increasing the density beyond the value $\rho_{x,1}^*$, an increasingly long segment of modes along the $\Gamma \rightarrow K$ branch goes unstable, as shown in Fig. 6.

3.2. Multiple occupancies and the optical branches

A multiply occupied crystal is a particular case of a Bravais lattice with a n_c -component basis, for which all basis vectors \mathbf{B}_i , $i = 1, 2, \dots, n_c$ are equal to zero. The displacement field $\mathbf{u}(\mathbf{R})$ has to be augmented to a ‘supervector’ $\{\mathbf{u}^{(\mu)}(\mathbf{R})\}$, $\mu = 1, 2, \dots, n_c$, where the superscript characterizes the particle species (all species and their interactions being identical in our case). The dynamical matrix in d spatial dimensions now becomes $dn_c \times dn_c$ and we obtain, accordingly, d acoustical and $d(n_c - 1)$ optical branches in the phonon spectrum.

For purposes of simplicity and transparency, we consider first, the case $d = 1$, i.e., a one-dimensional crystal of site occupancy n_c , formed by Q^\pm -particles. Due to the combination of the facts that all interactions between the species are identical *and* that all basis vectors vanish, it is straightforward to show that the $n_c \times n_c$ dynamical matrix $\mathbf{D}(k)$ takes, in this case, a special form of a Toeplitz matrix: all its diagonal elements

are equal to $A(k)$ and all non-diagonal ones to $B(k) \neq A(k)$, namely:

$$\mathbf{D}(k) = \begin{pmatrix} A(k) & B(k) & B(k) & B(k) & \cdot & \cdot & \cdot & B(k) \\ B(k) & A(k) & B(k) & \cdot & \cdot & \cdot & \cdot & B(k) \\ B(k) & B(k) & A(k) & \cdot & \cdot & \cdot & \cdot & B(k) \\ B(k) & \cdot & \cdot & \cdot & \cdot & \cdot & \cdot & \cdot \\ \cdot & \cdot & \cdot & \cdot & \cdot & \cdot & \cdot & \cdot \\ B(k) & B(k) & B(k) & \cdot & \cdot & \cdot & A(k) & B(k) \\ B(k) & B(k) & B(k) & \cdot & \cdot & \cdot & \cdot & A(k) \end{pmatrix}, \quad (13)$$

where

$$A(k) = \sum_R v''(R)[n_c - \cos(kR)] \quad (14)$$

$$B(k) = - \sum_R v''(R) \cos(kR), \quad (15)$$

and the summations in eqs. (14) and (15) are carried over all Bravais lattice vectors $\{R\}$. In the Appendix, we show that matrices of the form given by eq. (13) above have a highly degenerate eigenvalue spectrum and, in particular, one eigenvalue $\lambda_1 = A(k) + (n_c - 1)B(k)$ and $n_c - 1$ degenerate eigenvalues all equal to $\lambda_2 = A(k) - B(k)$. Introducing the specific expressions for $A(k)$ and $B(k)$ from eqs. (14) and (15), we obtain the phonon frequencies of the one-dimensional cluster crystal as:

$$\omega_1^2(k) = \frac{n_c}{m} \sum_R v''(R)[1 - \cos(kR)], \quad (16)$$

$$\omega_i^2(k) = \frac{n_c}{m} \sum_R v''(R), \quad i = 2, 3, \dots, n_c. \quad (17)$$

The first branch, eq. (16), is the acoustical one, whereas the remaining, $n_c - 1$ branches are not only all degenerate but they are also k -independent as well. This is a remarkable result that shows that cluster crystals are physical realizations of the Einstein phonon model. In addition, we observe that the squared frequencies scale linearly with the occupancy, n_c . The dependence on the density ρ of the crystal comes through the fact that the lattice vectors $\{R\}$, measured in units of the interaction range σ , change with concentration. We can thus write down the scaling relations for the acoustical and optical phonon frequencies, $\omega_{ac}(k; n_c, \rho)$ and $\omega_{op}(k; n_c, \rho)$ respectively, their dependence on the occupation number n_c and the density ρ of the crystal:

$$\omega_{ac}(k; n_c, n_c \rho) = \sqrt{n_c} \omega_{ac}(k; n_c = 1, \rho), \quad (n_c \geq 1) \quad (18)$$

$$\omega_{op}(k; n_c, n_c \rho/2) = \sqrt{\frac{n_c}{2}} \omega_{ac}(k; n_c = 2, \rho), \quad (n_c \geq 2) \quad (19)$$

As shown in sec. 2, the dependence of the lattice constant on density is rather weak and becomes increasingly suppressed as the density grows, as long as we stay within the limits of thermodynamic stability of the cluster crystals. Concomitantly, to an approximation that becomes more and more accurate as the density grows, we can state that having calculated the phonon spectra for some $n_c \gg 1$ is sufficient to accurately

predict the same for all higher values of n_c . Essentially, a single phonon spectrum for some lattice constant in the middle of the stability domain of the highly occupied crystal is, to zeroth-order approximation, the same for all densities in that regime and in going from the n_c - to the $n_c + 1$ -occupied crystal, one can simply take the frequencies and multiply them by the factor $\sqrt{(n_c + 1)/n_c}$ to obtain the new ones.

All these results carry over to arbitrary dimensions. The dynamical matrix of eq. (13) takes in d -dimensions a similar form, however the entries $A(k)$ and $B(k)$ become themselves $d \times d$ matrices $\mathbf{A}(\mathbf{k})$ and $\mathbf{B}(\mathbf{k})$ with entries:

$$A_{\alpha\beta}(\mathbf{k}) = \sum_{\mathbf{R}} \frac{\partial^2 v(\mathbf{R})}{\partial R_\alpha \partial R_\beta} [n_c - \cos(\mathbf{k} \cdot \mathbf{R})], \quad (20)$$

$$B_{\alpha\beta}(\mathbf{k}) = - \sum_{\mathbf{R}} \frac{\partial^2 v(\mathbf{R})}{\partial R_\alpha \partial R_\beta} \cos(\mathbf{k} \cdot \mathbf{R}), \quad (21)$$

where α, β are Cartesian coordinates and the summations run over all Bravais lattice vectors $\{\mathbf{R}\}$. The eigenvalue spectrum of this matrix is, as in the one-dimensional case, highly degenerate: a number $d(n_c - 1)$ of them, corresponding to the optical branches, are given by the difference of the diagonal elements of the block submatrices $\mathbf{A}(\mathbf{k})$ and $\mathbf{B}(\mathbf{k})$. For crystals of cubic symmetry, as is our case, we make use of the identity $\partial^2/\partial R_\alpha^2 = (1/d)\nabla^2$ for each Cartesian coordinate $\alpha = 1, \dots, d$, to find that the frequencies of the optical branches, ω_{op} , are given by the simple expression:

$$\omega_{\text{op}}^2 = \frac{n_c}{md} \sum_{\mathbf{R}} \nabla^2 \phi(\mathbf{R}), \quad (22)$$

where, as in the one-dimensional case, the frequencies are \mathbf{k} -independent and we obtain, once more, Einstein crystals. In fact, all optical modes are internal, “breathing modes” of the individual clusters on the lattice sites. In the acoustical oscillation modes, on the other side, all the particles within a given site move together as a composite object, i.e., the instantaneous displacements of all particles in a cluster are identical.

The result of eq. (22) above, has been anticipated in ref. [3] at the level of an approximation. There, the limit $n_c \gg 1$ has been considered, and the lattice oscillations have been modeled by deviations of a single particle from each of the lattice sites, while the remaining $n_c - 1$ ones remain approximately immobile, due to the large mass discrepancy between the two entities. That simplified approach results into an expression almost identical to eq. (22), with n_c being replaced by $n_c - 1$, the two quantities becoming arbitrarily similar in the region $n_c \gg 1$. In the same limit, it has been found that density functional theory predicts precisely the same dependence of the localization parameter of the one-particle density around the lattice sites. The phonon calculation performed here shows that all these features stem from the peculiar, Einstein-solid phonon spectrum of cluster crystals. In Fig. 7, we show as a concrete example the phonon spectrum of a doubly occupied GEM4 fcc crystal, featuring the acoustical and the triply degenerate optical branches.

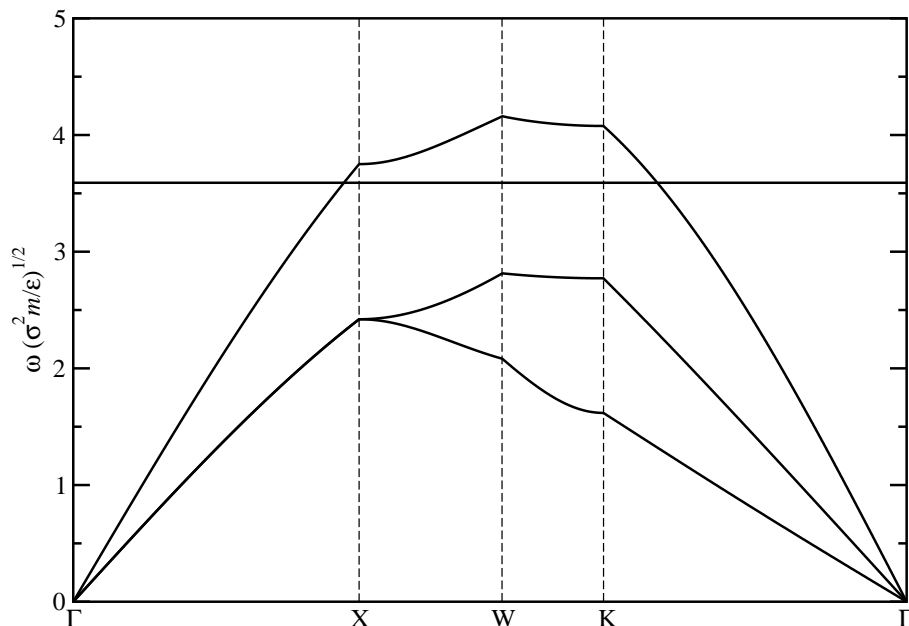


Figure 7. The phonon spectrum of the double occupied fcc GEM4-crystal at density $\rho^* = 1.0$. The thick vertical line is the triply degenerate optical branch.

3.3. Mechanical stability

We return now to the acoustical modes, to establish the existence of a cascade of mechanical instabilities in the system. Due to the inversion symmetry of the Bravais lattice, the acoustical modes of the crystal have low- k expansion that involves only even powers of the wavenumber:

$$\omega_{\text{ac}}^2(\mathbf{k}) = c_2(\hat{\mathbf{k}}; \rho, s)k^2 + c_4(\hat{\mathbf{k}}; \rho, s)k^4 + O(k^6), \quad (23)$$

with coefficients $c_i(\hat{\mathbf{k}}; \rho, s)$ that depend on the density ρ as well as the propagation direction $\hat{\mathbf{k}}$ and the branch index s .|| Stability against long-wavelength modulations means that the coefficient of the quadratic term, $c_2(\hat{\mathbf{k}}; \rho, s)$, must be positive for all directions and branches at a given density. Accordingly, a mechanical instability occurs at the point in which c_2 changes sign, the direction $\hat{\mathbf{k}}$ and the branch s for which this first occurs, as density grows, being the most unstable ones.

In sec. 3.1 we established the existence of a threshold density $\rho_{\times,1}^*$ for the single-occupied crystal, at which a mechanical instability occurs along the Γ K direction of the fcc GEM4-crystal; evidently, it holds $c_2(\hat{\mathbf{k}}; \rho_{\times,1}^*, s) = 0$ for the lowest branch in the Γ K-direction $\hat{\mathbf{k}}$ there. This fact, combined with the scaling relation, eq. (18), implies that there exist infinitely many mechanical instabilities, one for each occupancy n_c , and occurring at the corresponding threshold densities ρ_{\times,n_c}^* given by:

$$\rho_{\times,n_c}^* = n_c \rho_{\times,1}^*. \quad (24)$$

|| Note that the quantity $c_2(\hat{\mathbf{k}}; \rho, s)$ is the squared speed of sound of the s -branch for propagation along the $\hat{\mathbf{k}}$ direction. For completeness, we also note that an expansion of the form of eq. (23) holds true for the optical modes as well, with the addition of a term $c_0(\hat{\mathbf{k}}; \rho, s)$.

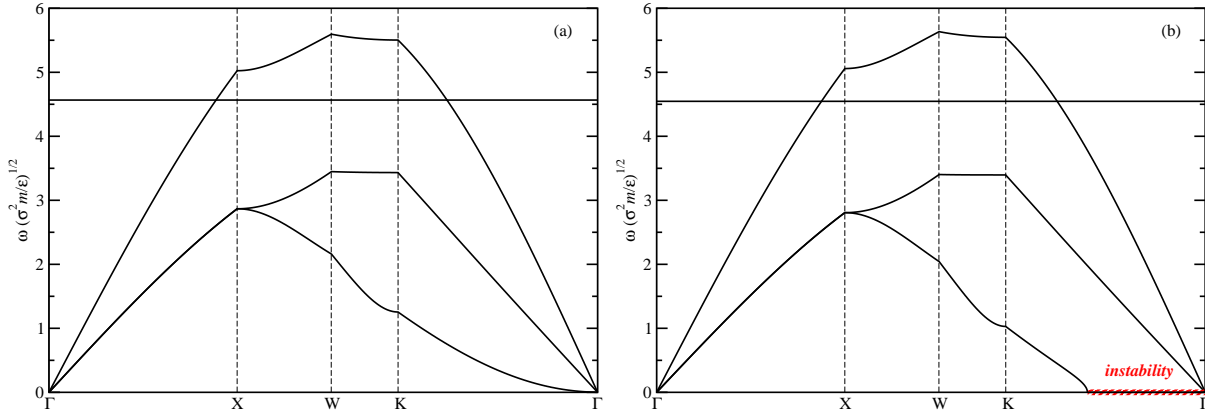


Figure 8. (a) The phonon spectrum of the fcc GEM4 double occupied crystal at the threshold density $\rho_{X,2}^* = 1.441$. Note the dependence $\omega(k) \propto k^2$ of the lowest-lying acoustical branch along the Γ K direction. (b) The same at a density beyond the threshold value, $\rho^* = 1.5$, where a whole region, marked by the cross-hatched symbols, has become unstable.

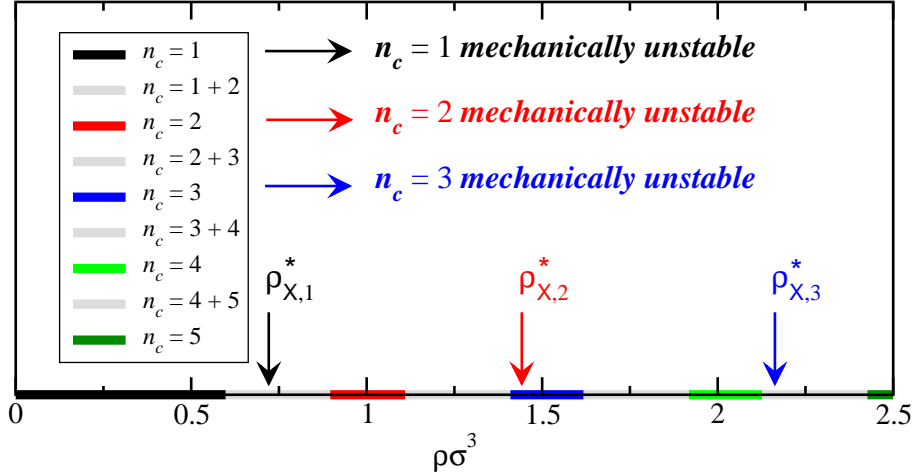


Figure 9. The regions of stability of the pure, n_c -occupied GEM4-crystals at $T = 0$, as indicated in the legend, are shown together with the coexistence regions (marked gray) and the threshold densities ρ_{X,n_c}^* of mechanical stability marked by the arrows. The latter are color-coded in the same way as the thermodynamic stability regions of the n_c -occupied crystals.

We have numerically confirmed this prediction for GEM4-crystals of a few low occupancies and we show, as a representative result, in Fig. 8 the phonon spectra of double occupied GEM4-crystals exactly at the threshold density $\rho_{X,2}^*$, and at a slightly higher one where a number of modes feature imaginary frequencies.

In Fig. 9 we graphically summarize the zero-temperature thermodynamic and stability phase diagrams for the GEM4-model, showing the sequence of the first few occupancies for the fcc crystals. It can be seen that the instability densities ρ_{X,n_c}^* of the n_c occupied crystals occur well beyond the limits of their thermodynamic stability.

The existence of the former can be understood in terms of the particular form of the interaction potential. Suppose we restrict ourselves to single occupied crystals and we increase the density. This compresses the system, causing the lattice constant to shrink. Since the interaction potential contains a flat part at small separations, and in view of the fact that the restoring forces in the crystal come mainly from the nearest neighbors, at some threshold value of the shrinking lattice constant the restoring force will vanish, at least along one crystallographic direction (in our case, along the nearest-neighbor vector). This signals the mechanical instability. Now, *the same* argument carries over to a crystal of occupancy n_c at n_c times the threshold density of the single occupied crystal, since the two are copies of each other as far as the lattice constant is concerned and only the forces in the latter are n_c times bigger than the ones in the former. If the restoring force in some direction of the single occupied crystal vanishes, it will also do so at the same direction for the n_c occupied crystal. We see, therefore, that the whole cascade of isostructural transitions is a straightforward consequence of the transition from the single to the double occupancy, which can be seen as the strategy of the system to avoid the mechanical collapse. Indeed, multiple occupancy allows the system to readjust its lattice constant and to arrange the particles in such a way that all restoring forces are nonvanishing, offering the solid stability against thermal fluctuations. The fact that the thermodynamic phase transitions preempt the mechanical ones is reassuring and in line with a number of other examples, in which a system undergoes a first-order transition that has an instability line deep in the region of the two-phase coexistence (or even beyond it, as in our case). The existence of the instability, however, has implications on the nucleation rates of the multiply occupied crystals, since, as one approaches it, it becomes exceedingly difficult to maintain thermodynamically metastable crystals of the wrong occupancy, a feature that should drastically suppress the corresponding nucleation barriers.

4. Phonon thermodynamics and isostructural critical points

Up to now our considerations were limited to $T = 0$ and to mechanical equations of motion of the particles around their equilibrium positions. Here we will reintroduce finite temperatures and calculate free energies and the ensuing phase diagrams that follow on the basis of phonon modes *alone*.

The normal modes render the harmonic part of the system's Hamiltonian diagonal, i.e., a decoupling among the modes results. In a crystal with N particles, occupancy per site n_c and N_ℓ lattice sites, we have $N = n_c N_\ell$. The original coordinates are the $3N$ Cartesian displacements of the particles from their equilibrium sites. In the normal mode description, these are replaced by $3n_c$ branches, each one containing N_ℓ values of the wavevector \mathbf{k} compatible with the Born-von Karman boundary conditions, giving rise, consistently, to $3n_c N_\ell = 3N$ coordinates, as in the original description. The Helmholtz free energy F of the harmonic solid takes, after the introduction of the normal modes,

and on the basis of the decoupling among them, the simple form:

$$\frac{F}{V} = \frac{U}{V} + \frac{k_B T}{(2\pi)^3} \sum_{s=1}^{3n_c} \int' d^3k \ln \left[\frac{\hbar\omega_s(\mathbf{k})}{k_B T} \right], \quad (25)$$

which includes the contributions from the momentum degrees of freedom as well as the zero-point energy U (the lattice sum) of the crystal. In eq. (25) above, the integral over k extends within the first Brillouin zone of the crystal, a fact indicated by the prime, whereas the sum runs over the $3n_c$ branches of the phonon spectrum, characterized by the dispersion curves $\omega_s(\mathbf{k})$.

Let us now focus on the limit $n_c \gg 1$. Here, the $3(n_c - 1)$ optical branches dominate over the three acoustical ones, so we ignore the latter in what follows,[¶] and we further make the approximation $n_c - 1 \cong n_c$. Since the optical frequencies ω_{op} are \mathbf{k} -independent, we can pull the whole integrand out of the integral in eq. (25) above. The remaining integral $(2\pi)^{-3} \int' d^3k$ yields the density of *lattice sites*, N_ℓ/V , whilst the summation over s gives the number $3n_c$ of phonon branches; the two combine into $3n_c N_\ell/V = 3N/V = 3\rho$, to give, within the stated approximations:

$$\frac{F}{V} = \frac{U}{V} + 3k_B T \rho \ln \left[\frac{\hbar\omega_{\text{op}}}{k_B T} \right]. \quad (26)$$

Apart from the manifest ρ -dependence of the second term on the right-hand-side of eq. (26), there is an implicit one through the optical frequency ω_{op} ; an explicit expression for the latter is given in eq. (22). The density enters there through the dependence of n_c and the lattice vectors $\{\mathbf{R}\}$ on ρ . As discussed in length in sec. 2, at the limit $n_c \gg 1$ considered here, the lattice constant can be taken as density independent, due to the approximate property $n_c \propto \rho$. Accordingly, we define the ρ -independent frequency $\omega_0^2 = \sum_{\mathbf{R}} \nabla^2 \phi(\mathbf{R}) / (3m)$, for which the set of lattice vectors $\{\mathbf{R}\}$ is determined by the interparticle interaction *alone* and, in particular, by the property that the length of the shortest reciprocal lattice vector of the crystal coincides with k_* , the wavenumber at which $\tilde{v}(k)$ has its most negative amplitude [3]. Then, we have $\omega_{\text{op}} \cong \sqrt{n_c} \omega_0$ and its ρ -dependence comes exclusively through n_c , for which we know that $n_c \propto \rho$. Gathering all the results together, introducing them into eq. (26), and absorbing all terms linear in ρ into a separate term with some proportionality constant C , we arrive at the result:

$$\frac{F}{V} \cong \frac{U}{V} + \frac{3k_B T}{2} \rho \ln(\rho \sigma^3) + C\rho, \quad (27)$$

where we have introduced an arbitrary length scale σ in the logarithm to render its argument dimensionless. The last term, $C\rho$, has no effect on the determination of phase boundaries; it acts simply as a constant shift to the chemical potential, leaving the pressure invariant, thus it will be dropped in what follows. We arrive, thus, at a remarkably simple (albeit approximate) result, eq. (27), which states that the phonon free energy of the cluster crystals can be expressed as the sum of the ground state energy U plus an ideal gas contribution, the latter corresponding to a ‘fictitious temperature’ equal to three-halves the real one.⁺

[¶] The acoustical branches can also be taken into account analytically, within the Debye approximation.

⁺ In d spatial dimensions this would be d -halves the real temperature.

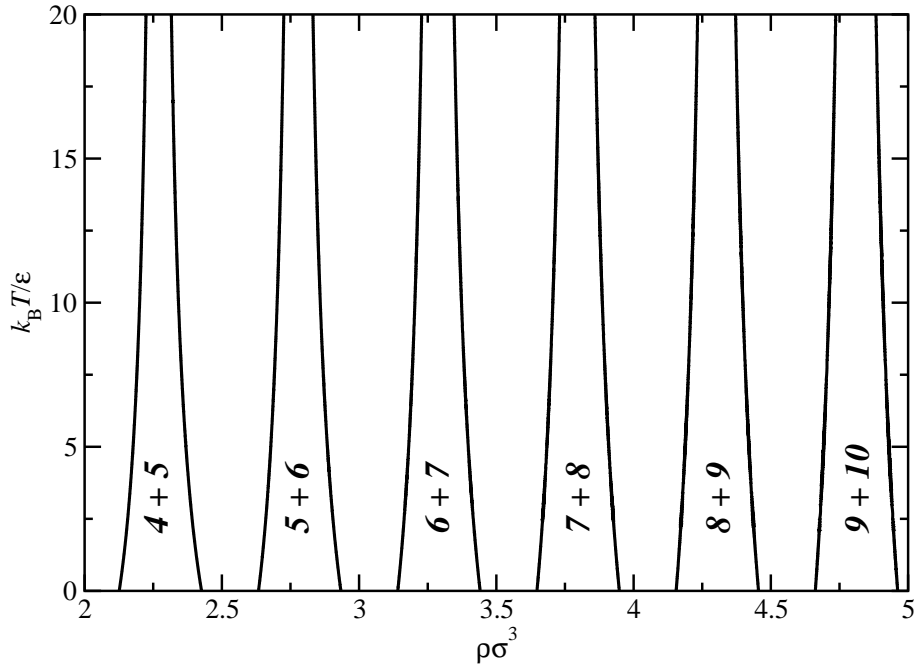


Figure 10. The phonon-based phase diagram of the GEM4-model, shown here, in part, for the region of moderate occupancies, for which the theoretical approximations discussed in the text are becoming increasingly valid. Two-phase regions of coexistence between fcc crystals of occupancy n_c and $n_c + 1$ are indicated by the inscriptions, whereas unlabeled domains correspond to single-phase regions. The coexistence density gaps found at $T = 0$ are being narrowed as T grows, due to phonon contributions, but they never close. In the true phase diagram, hopping processes eliminate regions of stability of crystals with different site occupancies at sufficiently high temperatures.

We can now, on the basis of the free energy of eq. (27) above draw a *phononic* phase diagram of the crystal states of the system. The qualification pertains to the fact that in writing down eq. (27), the contributions from the phonons *only* have been taken into account. Both the disturbances of the phonon spectra arising from imperfect crystals with nonuniform site occupancies and the entropy associated with hopping are *not* included in the free energy of eq. (27). The first term there simply gives the $T = 0$ phase diagram with the phase coexistence regions discussed in sec. 2. The second term, seen as a function of ρ , has curvature $3k_B T / (2\rho) > 0$, thus it will act to narrow the width of the density gaps as temperature grows.

The phase diagram can be drawn by performing the double tangent construction on the F/V vs. ρ -curves and it is shown in Fig. 10 for a region of moderate values of the density and thus site occupation numbers. As anticipated above, the phonon contributions lead to a narrowing of the density gaps as temperature increases. Nevertheless, the crystals of different occupancy remain distinct at all temperatures, as is natural for an approach that does not allow hopping and smooth adjustments of the lattice constant. The phonon-based phase diagram of Fig. 10 must now be juxtaposed to the ‘exact’ one, arising from density functional theory [3, 2, 4] and

computer simulations [10]. The full phase diagram is free of the coexistence regions between crystals of different occupancy, for temperatures at least as high as $T^* = 0.1$. Evidently, all the contributions from hopping, inhomogeneous lattice site occupancy and anharmonicities, bring about the effect of ‘washing out’ the step-like behavior of n_c and thus eliminating the first-order phase transitions between crystals of different site occupancies at sufficiently high temperatures. On the other hand, at $T = 0$ the density gaps and the transitions between such crystals are definitely present. Whichever contribution hopping and anharmonicities have on the free energy, it cannot simply eliminate the gaps present at $T = 0$ for arbitrarily small temperatures. It follows that the only possibility to reconcile the low- and high-temperature properties of the model is to put forward the conjecture that the coexistence gaps between crystals of occupancy n_c and crystals of occupancy $n_c + 1$ must narrow down as T grows and terminate at critical points. As there are infinitely many gaps at $T = 0$, it follows that the system must feature infinitely many, low- T critical points at which the isostructural fcc-fcc transitions end. Preliminary simulations seem to confirm this hypothesis [17], whereby the critical temperature T_c has been estimated in the order of magnitude $k_B T_c / \varepsilon \sim 10^{-2}$.

The isostructural fcc-to-fcc transitions and their termination at a critical point bear some similarities to the ones discovered, and extensively investigated, in the 1990s for hard-sphere systems with short-range attractive or repulsive interactions [18, 19, 20, 21, 22, 23, 24, 25, 26, 27]. Also in that case, two fcc-lattices with different values of the lattice constant were found to coexist at sufficiently low temperatures, the difference between the two gradually disappearing as the temperature grows. There are, however, a number of important differences. First, in the previous cases, the coexistence was not a ground-state feature, since it disappeared below the triple, fcc-fcc-gas temperature, to give its place to a usual, fcc-gas coexistence. Second, the two crystals had the same occupancy there, unity, whereas here they are characterized by different values of n_c . Finally, the systems at hand present *infinitely many* such regions of coexistence and corresponding critical temperatures, as opposed to a single one in previous models.

5. Summary and conclusions

We have investigated the ground states and the phonon spectra of cluster crystals formed by Q^\pm -particles, finding a cascade of isostructural transitions and the emergence of these systems as realizations of Einstein crystals. We have put forward the hypothesis that the systems display infinitely many, low-temperature critical points in which the fcc-fcc transitions terminate. The predictions made here hold quite generally for all Q^\pm potentials, *provided* there exist mutual, nonvanishing forces between the particles, so that the arguments presented in sec. 2 hold. An important exception is the so-called penetrable sphere model (PSM) [28], which is formally a GEM with infinite exponent, and for which no forces act between the particles; consequently, neither the ground state requires a vanishing force on each particle due to its neighbors nor is a harmonic

expansion of the potential possible. For the PSM, the low-temperature phase diagram features *gradual* crossovers from low- to high-occupancy fcc-crystals instead [28].

Finally, we comment on the possible limitations of our simplifying assumption that in any given solid at $T = 0$ all sites have the same, integer occupancy n_c . As discussed in sec. 2, the occupancy can be at most a rational number. Therefore, even in full generality, isostructural transitions between rationally occupied crystals would appear – the rational numbers forming a discrete set, as opposed to the general, real occupancy found by density functional theory and simulation at moderate and high temperatures. It follows that the conclusions on the necessity to terminate the isostructural transitions at critical points remain unaffected.

Acknowledgments

The authors acknowledge useful discussions with Ronald Blaak, Bianca Mladek, Daniele Coslovich, Lukas Strauss, Gerhard Kahl, and Daan Frenkel.

Appendix

Consider a $\nu \times \nu$ Toeplitz matrix \mathcal{M}_ν with the property that all its diagonal elements are equal to A and the nondiagonal ones equal to B , i.e.:

$$\mathcal{M}_\nu = \begin{pmatrix} A & B & B & \dots & B \\ B & A & B & \dots & B \\ B & B & A & \dots & B \\ B & & & \dots & B \\ B & & & \dots & B \\ B & & & \dots & B \\ B & B & B & \dots & A \end{pmatrix}, \quad (28)$$

Replacing the first diagonal element of \mathcal{M}_ν with B we obtain the matrix $\bar{\mathcal{M}}_\nu$ with the form:

$$\bar{\mathcal{M}}_\nu = \begin{pmatrix} B & B & B & \dots & B \\ B & A & B & \dots & B \\ B & B & A & \dots & B \\ B & & & \dots & B \\ B & & & \dots & B \\ B & & & \dots & B \\ B & B & B & \dots & A \end{pmatrix}, \quad (29)$$

The following statements hold true for the determinants $|\mathcal{M}_\nu|$ and $|\bar{\mathcal{M}}_\nu|$ of the two matrices:

$$|\mathcal{M}_\nu| = (A - B)^{\nu-1}[A + (\nu - 1)B]; \quad (30)$$

$$|\bar{\mathcal{M}}_\nu| = B(A - B)^{\nu-1}. \quad (31)$$

The proof follows by induction. Evidently, the relations hold for $\nu = 2$. Now assume that they hold for $\nu = n$. Developing the determinant of the matrices \mathcal{M}_{n+1} and $\bar{\mathcal{M}}_{n+1}$ around the entries of their first rows, we obtain:

$$|\mathcal{M}_{n+1}| = A|\mathcal{M}_n| - nB|\bar{\mathcal{M}}_n|; \quad (32)$$

$$|\bar{\mathcal{M}}_{n+1}| = B|\mathcal{M}_n| - nB|\bar{\mathcal{M}}_n|. \quad (33)$$

Introducing into eqs. (32) and (33) the expressions of eqs. (30) and (31), assumed valid for $\nu = n$, results into the relations, now proven valid for $\nu = n + 1$:

$$|\mathcal{M}_{n+1}| = (A - B)^n(A + nB); \quad (34)$$

$$|\bar{\mathcal{M}}_{n+1}| = B(A - B)^n, \quad (35)$$

which completes the proof.

The characteristic polynomial $p_\nu(\lambda)$ of the matrix \mathcal{M}_ν is, due to the special form of the latter, obtained through the formal substitution $A \rightarrow A - \lambda$ in the expression for $|\mathcal{M}_\nu|$. Accordingly, the eigenvalue equation $p_\nu(\lambda) = 0$ reads, for this matrix, as:

$$(A - B - \lambda)^{\nu-1}[A + (\nu - 1)B - \lambda] = 0, \quad (36)$$

from which the eigenvalue spectrum of the matrix \mathcal{M}_ν follows as:

$$\lambda_1 = A + (\nu - 1)B; \quad (37)$$

$$\lambda_i = A - B. \quad (i = 2, 3, \dots, \nu) \quad (38)$$

The second equation manifests the degeneracy of $\nu - 1$ eigenvalues of the matrix.

References

- [1] Likos C N, Lang A, Watzlawek M and Löwen H 2001 *Phys. Rev. E* **63** 031206
- [2] Mladek B M, Gottwald D, Kahl G, Neumann M and Likos C N 2006 *Phys. Rev. Lett.* **96** 045701
- [3] Likos C N, Mladek B M, Gottwald D and Kahl G 2007 *J. Chem. Phys.* **126** 224502
- [4] Mladek B M, Gottwald D, Kahl G, Neumann M and Likos C N 2007 *J. Phys. Chem. B* **111** 12799
- [5] Glaser M A, Grason G M, Kamien R D, Košmrlj A, Santangelo C D and Zihlerl P 2007 *EPL* **78** 46004
- [6] Sütő A 2005 *Phys. Rev. Lett.* **95** 265501
- [7] Sütő A 2006 *Phys. Rev. B* **74** 104117
- [8] Likos C N 2006 *Nature* **440** (7083) 433
- [9] van Teeffelen S, Moreno A J and Likos C N 2009 *Soft Matter* **5** 1024
- [10] Mladek B M, Charbonneau P and Frenkel D 2007 *Phys. Rev. Lett.* **99** 235702
- [11] Mladek B M, Charbonneau P, Likos C N, Frenkel D and Kahl G 2008 *J. Phys.: Condens. Matter* **20** 494245
- [12] Mladek B M, Kahl G and Likos C N 2008 *Phys. Rev. Lett.* **100** 028301
- [13] Narros A, Moreno A J and Likos C N 2010 *Soft Matter* **6** 2435
- [14] Moreno A J and Likos C N 2007 *Phys. Rev. Lett.* **99** 107801
- [15] Gottwald D, Kahl G and Likos C N 2005 *J. Chem. Phys.* **122** 204503
- [16] Ashcroft N W and Mermin N D 1976 *Solid State Physics* (Philadelphia, PA: Holt Saunders)
- [17] Zhang K, Charbonneau P and Mladek B M *unpublished*
- [18] Young D A and Alder B J 1980 *J. Chem. Phys.* **73** 2430
- [19] Bolhuis P and Frenkel D 1994 *Phys. Rev. Lett.* **72** 2211
- [20] Bolhuis P, Hagen M and Frenkel D 1994 *Phys. Rev. E* **50** 4880

- [21] Likos C N, Németh Z T and Löwen H 1994 *J. Phys.: Condens. Matter* **6** 10965
- [22] Rascón C, Navascués G and Mederos L 1995 *Phys. Rev. E* **51** 14899
- [23] Rascón C, Mederos L and Navascués G 1996 *Phys. Rev. Lett.* **77** 2249
- [24] Likos C N and Senatore G 1995 *J. Phys.: Condens. Matter* **7** 6797
- [25] Németh Z T and Likos C N 1995 *J. Phys.: Condens. Matter* **7** L573
- [26] Rascón C, Mederos L and Navascués G 1995 *J. Chem. Phys.* **103** 9795
- [27] Lang A, Kahl G, Likos C N, Löwen H and Watzlawek M 1999 *J. Phys.: Condens. Matter* **11** 10143
- [28] Likos C N, Watzlawek M and Löwen H 1998 *Phys. Rev. E* **58** 3135